On the influence of moisture on the strength of thermals:
A large-eddy simulation case study

Oliver Maas and Dieter Etling

`maas@meteo.uni-hannover.de`

Institute of Meteorology and Climatology, Leibniz Universität Hannover, Hanover, Germany

Abstract

Thermals in the atmosphere are driven by buoyancy forces due to density differences between air parcels and their environment (Archimedes principle). Here we present some estimates on the contribution of moisture on the strength of thermals based on numerical simulations with a large-eddy-simulation model (LES).

Nomenclature

A	vertical acceleration of an air parcel $[m/s^2]$
B	buoyancy force per unit volume $[N/m^3]$
B_s	surface buoyancy flux $[Km/s]$
Bo	Bowen ratio [-]
c_p	specific heat of air $[1004 J/(kgK)]$
g	acceleration due to gravity $[9.81\,m/s^2]$
p	air pressure $[Pa]$
q	specific humidity [-]
Q	total heat flux $[W/m^2]$
Q_l	latent heat flux $[W/m^2]$
Q_s	sensible heat flux $[W/m^2]$
R	universal gas constant $[287.04\,J/(kgK)]$
T	temperature $[K]$
T_v	virtual temperature $[K]$
w_*	convective velocity scale $[m/s]$
z_i	inversion layer height $[m]$
θ	potential temperature $[K]$
θ_v	virtual potential temperature $[K]$
ρ	air density $[kg/m^3]$
$()'$	deviation from the horizontal mean
$()_p$	index for an air parcel
$()_e$	index for the environment

Introduction

There has been some debate in recent years within the soaring community on the contribution of atmospheric moisture content on thermals, especially if moisture might be even the dominating factor on thermal strength. The arguments are based mainly on measurements of temperature and moisture (in terms of specific humidity) inside and outside thermals obtained by gliders and

aircrafts equipped with instruments [1], [2], [3]. But as the temperature and moisture differences between thermals and their environment are quite small, this question has not been answered by measurements without doubt. Here we present a complementary approach based on numerical simulations for a field of thermals in the atmospheric boundary layer as heated from below. The method is to apply a so-called Large-Eddy-Simulation model (LES) which resolves the largest eddies in the convective atmospheric boundary layer [4], [5]. In order to quantify the effect of the moisture content of rising thermals on the vertical velocity (updrafts), vertical profiles of temperature and specific humidity have been varied systematically by applying different values for latent heat flux (moisture flux) and sensible heat flux (temperature flux) as forcing at the earth surface. In order to quantify the contribution of moisture on the strength of thermals, various data on temperature, specific humidity and vertical velocity have been extracted from the 3-D simulations. The influence of moisture on the structure of the convective boundary layer has been also investigated by Patton et al. [6]

The influence of moisture in Archimedes principle

The vertical acceleration (A) of air parcels in the atmosphere is based on Archimedes principle which can be formally expressed by the buoyancy force (B) as:

$$B = \rho_p A = -g\left(\rho_p - \rho_e\right),\qquad(1)$$

where g is gravity, ρ_p the density of an air parcel and ρ_e the density of its environment. $A = dw/dt$, where w is the vertical velocity and t is time. The air density ρ is defined by air pressure p, air temperature T and moisture content (specific humidity q) through the ideal gas law:

$$p = R\rho\left(1 + 0.6q\right)T.\qquad(2)$$

where R is the universal gas constant. Inserting (2) in (1), the vertical acceleration can be expressed by air temperature T and
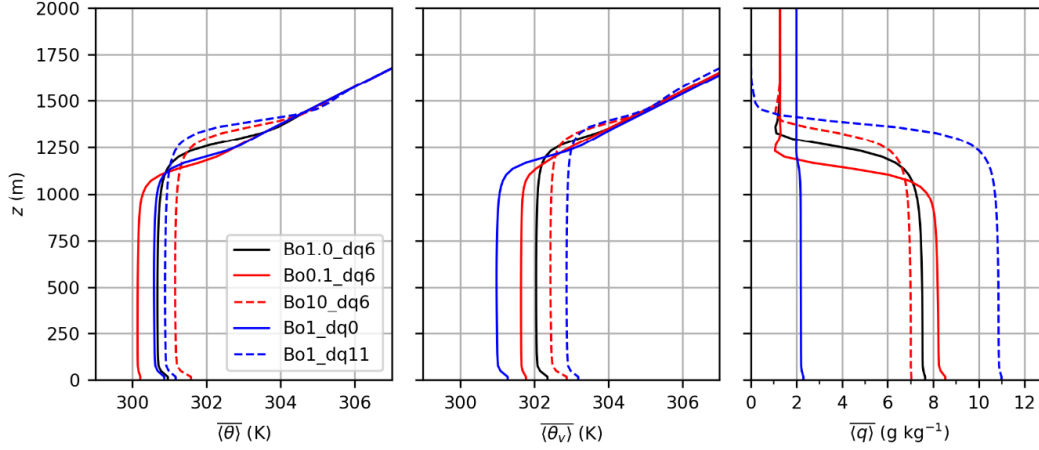
Fig. 1: Horizontal and temporal averaged profiles of potential temperature θ, virtual potential temperature θ_v and specific humidity q for the five cases Bo1.0_dq6 (reference), Bo0.1_dq6 (wet surface), Bo10_dq6 (dry surface), Bo1_dq0 (no humidity difference between the Boundary Layer (BL) and the Free Atmosphere (FA)) and Bo1_dq11 (high humidity difference between BL and FA).

specific humidity q approximately by:

$$A = g\,\frac{(T_p - T_e)}{T_e} + g\,0.6\,(q_p - q_e) = A_t + A_q. \tag{3}$$

It is common to combine the last two terms in (2) to form the so-called virtual temperature T_v:

$$T_v = (1 + 0.6q)\,T. \tag{4}$$

By using (4), the vertical acceleration A provided by buoyancy forces (3) can also be written as:

$$A = g\,\frac{(T_{vp} - T_{ve})}{T_{ve}}. \tag{5}$$

In a dry atmosphere ($q = 0$), thermals are driven by the temperature differences between the thermal and its environment, where updrafts are generated for $T_p > T_e$. In a moist atmosphere ($q > 0$), moisture differences between thermals and their environment provide an additional acceleration, where updrafts are supported for ($q_p > q_e$), i.e. air parcels are moister than their environment. To provide an example of the magnitudes of the vertical acceleration due to temperature differences (A_t) and due to moisture differences (A_q) let us assume typical values as found in moist thermals (see Fig. 4): $T_p - T_e = 0.2\,K$, $q_p - q_e = 0.2\,g/kg = 0.0002$. Then we have: $A_t = 0.007\,m/s^2$, $A_q = 0.0012\,m/s^2$ and $A_q/A = 0.15 = 15\%$. Hence moisture (specific humidity) contributes to the strength of thermals but is not the dominating factor. In meteorology it is also common to introduce a new temperature measure called "potential temperature", designated by the Greek symbol θ which is related to air temperature T by:

$$\theta = T\,\left(\frac{p_0}{p}\right)^{\kappa}, \tag{6}$$

where $p_0 = 1000\,hPa$ and $\kappa = 0.262$.

The potential temperature is a conserved quantity for adiabatic processes e.g. for an ascending air parcel θ is constant whereas temperature T is decreasing with height. Hence the vertical stratification in the atmosphere can be easily identified by profiles of θ, as $\theta(z)$ is constant for adiabatic (neutral) stratification, decreases with height in unstable conditions and is increasing for stable stratification. Examples for profiles of potential temperature θ and virtual potential temperature θ_v are displayed in Fig 1.

Numerical Setup

The numerical simulations were conducted with the **PA**rallelized **L**arge-eddy simulation **M**odel **PALM**, developed at the Leibniz University Hannover, Germany [7]. Classical simulation methods, that are e.g. used for the numerical weather forecast, only simulate the mean flow, such as the mean wind speed and mean temperature profile. Large-eddy simulation (LES), however, is a simulation method that explicitly resolves the largest eddies (turbulent motions) of the turbulent lower atmosphere, i.e. the boundary layer (BL). Hence, the properties of updrafts and downdrafts can be investigated.

The simulations are initialized with potential temperature θ and specific moisture q being constant up to the inversion height z_i (about $1000\,m$), hence the BL is neutrally stratified with respect to temperature as well with respect to moisture. Above z_i a stably stratified free atmosphere (FA) is prescribed with $\theta(z)$ increasing with height by $1\,K/(100\,m)$ and a moisture jump Δq with dryer FA above (see Fig. 1). The development of vertical profiles of temperature and moisture with time is forced by applying a sensible heat flux (Q_s) and a latent heat flux (Q_l) at the earth surface. These fluxes have to compensate energy fluxes due to incoming solar radiation, the ground heat flux and netlongwave radiation in order to fulfil the energy balance at the earth surface. As sensible heat flux is related to air temperature and latent heat flux to evaporation, Q_s might also be called tem-
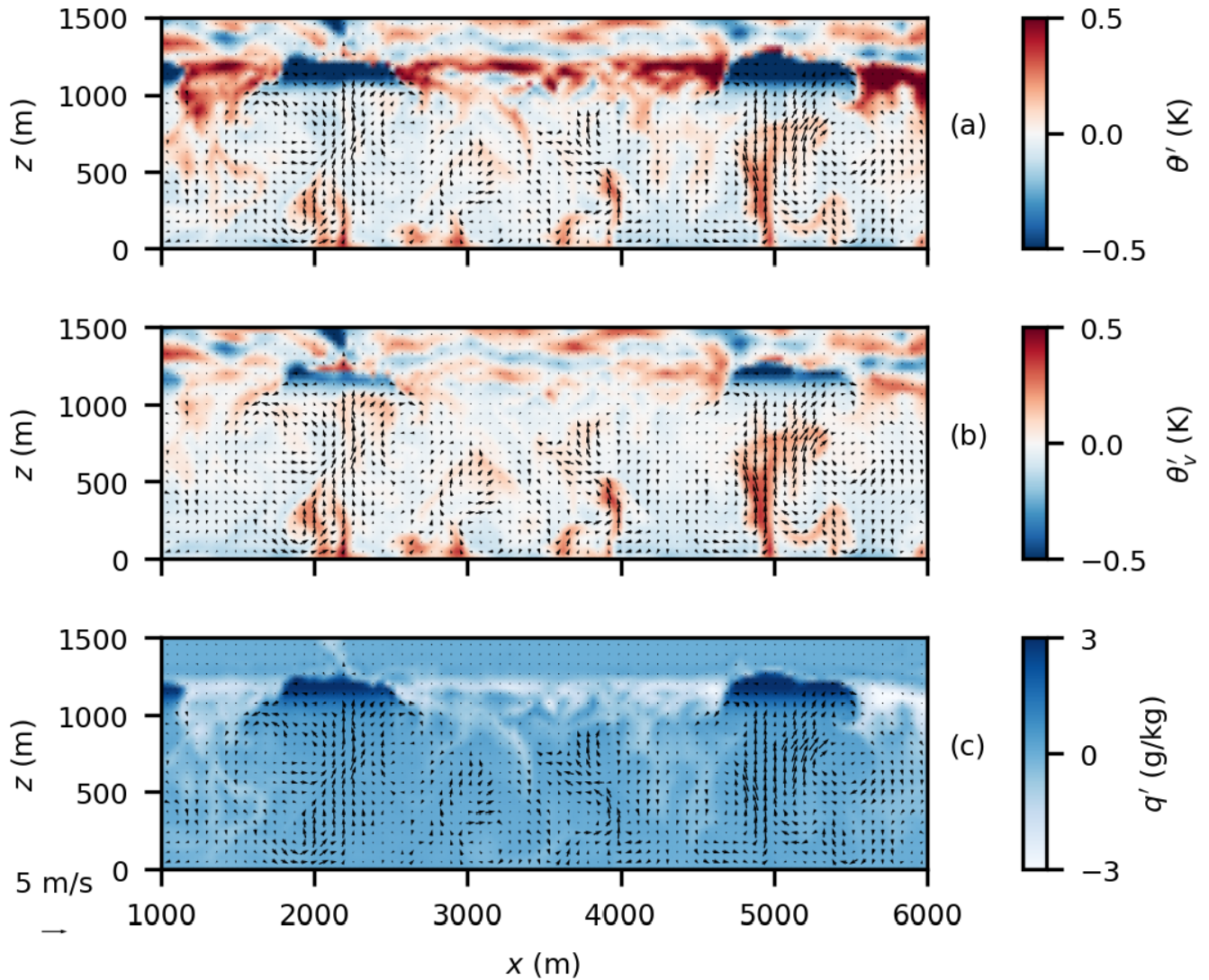
Fig. 2: Vertical cross sections of potential temperature excess θ' (a) (click here for animation) , virtual potential temperature excess θ'_v (b) and specific humidity excess q' (c) (click here for animation) for the case Bo1_dq6 (arrows indicate flow velocity)

perature flux and Q_l named moisture flux. The input of heat and moisture fluxes at the surface of a neutrally stratified BL is leading the formation of unstably stratified temperature and moisture profiles (see Fig. 1), hence initiating thermal convection in the form of rising thermals (see Fig. 2).

In micrometeorology, the relation between sensible heat flux and latent heat flux is called Bowen ratio, defined as

$$Bo = Q_s/Q_l. \tag{7}$$

A large Bowen ratio occurs if the surface is dry and most of the heat flux is used to heat up the near-surface air. A small Bowen ratio represents a wet surface and most of the heat flux is used for evaporation of water, so that the humidity of the near-surface air increases. In nature, a large variety of combinations for sensible and latent heat flux can be observed, even for the

same Bowen ratio. In order to restrict our simulations to a few simple cases, we performed all runs with the same total heat flux $Q = Q_s + Q_l = 200\,W/m^2$ and varied within this limit the Bowen ratio between 0.1 and 10 (see Table 1).

The humidity difference between the BL and the FA is varied from $0\,g/kg$ to $11\,g/kg$, as can be seen in the profiles of specific humidity in Fig. 1. The domain size in all cases is $L_x = 8192\,m$, $L_y = 5120\,m$ and $L_z = 3300\,m$, so that several convection cells fit into the domain. The grid spacing is $32\,m$ in all directions, which is enough to resolve thermals that have a typical diameter of several $100\,m$. Cyclic boundary conditions are applied at the lateral boundaries. A Rayleigh damping layer at the top of the domain prevents the reflection of gravity waves that are triggered by thermals penetrating the inversion layer. Monin-Obukhov similarity is assumed between the surface and the lowest grid level.

Case	Bo	Δq g/kg	w_* m/s	z_i m	z_T m	z_B m	$\frac{z_T}{z_i}$	$\frac{z_B}{z_i}$	$\frac{z_B - z_T}{z_i}$
Bo1_dq6	1	6	1.54	1296	941	1106	0.73	0.85	0.12
Bo0.1_dq6	0.1	6	0.99	1168	664	958	0.57	0.82	0.25
Bo10_dq6	10	6	1.87	1360	1091	1203	0.80	0.88	0.08
Bo1_dq0	1	0	1.51	1200	984	997	0.82	0.83	0.01
Bo1_dq11	1	11	1.58	1392	1014	1201	0.73	0.86	0.13

Table 1: Overview of the five simulated cases with Bowen ratio Bo, specific humidity difference between BL and FA Δq, typical updraft velocity w_* (convective velocity scale), inversion height z_i, height at which updrafts ($w > w_*$) have zero temperature excess z_T) or have zero buoyancy z_B.

The simulations ran for 2 hours physical time, the profiles are averaged over the last 15 minutes and the vertical cross sections are obtained from the last time step. In order to keep this investigation simple, we choose the basic temperature and humidity profiles in such a way that no condensation of water vapor will occur within the BL, hence no cumulus clouds will form. In such a way we can investigate the pure effect of moisture content in the BL on buoyancy forces and hence on thermals. Of course, if condensation would be permitted, the release of latent heat would lead to additional buoyancy in the thermals at condensation level and the updrafts will become stronger than in the case without cloud formation. We also assume that there is no background wind.

The simulations can be performed on a modern notebook, given this grid spacing and domain size. Note that [4] used a similar domain size and grid spacing for their large-eddy simula-
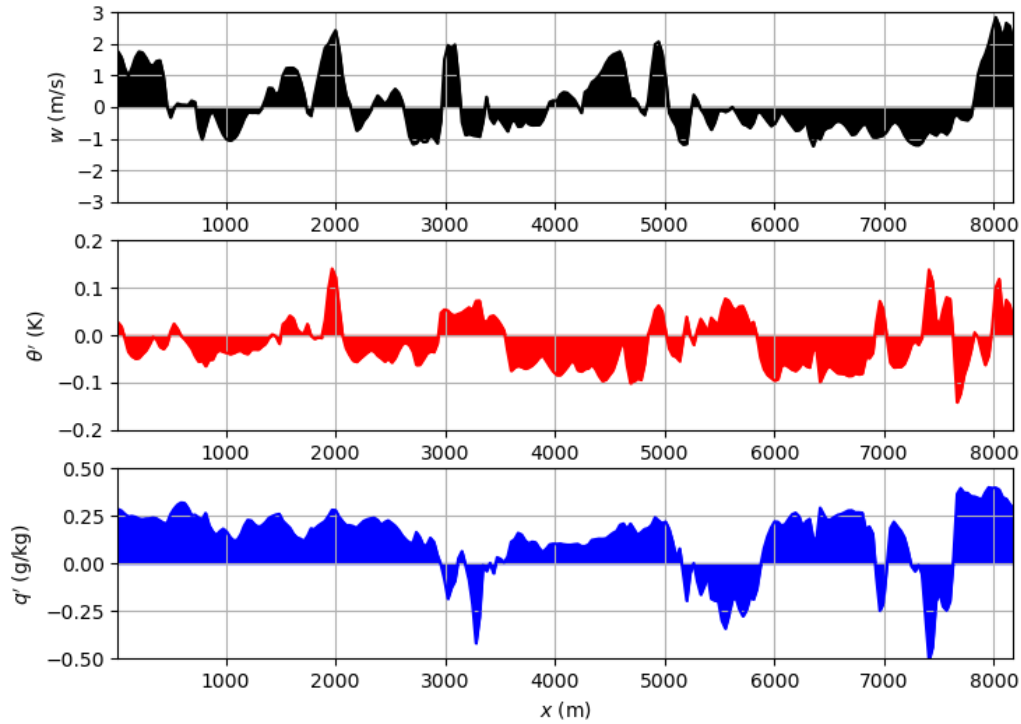

Fig. 3: Vertical velocity w, potential temperature difference θ' and specific humidity difference q' along a horizontal transect located at $y = 16m$, $z = 816m$.

tion study and that a supercomputer was required for performing the simulations in the year 1989.

Results

Figure 2 shows vertical cross sections of potential temperature, virtual potential temperature and specific humidity as deviations (θ', θ_v', q') from the respective horizontal mean value for the case Bo1_dq6 (dry surface). Two large updrafts with a distance of about $2.3\,z_i$ can be identified. As can be seen in Fig. 2a, these updrafts are relatively warm near the surface, but are relatively cold near the top of the BL. Figure 2c shows that the humidity excess of updrafts is highest at the top of the BL but it is nearly zero near the surface. The high humidity differences q' at the top of the updrafts adds buoyancy so that relatively cold updrafts (negative θ') can still be positively buoyant (positive θ_v'). Beside the updrafts, warm and dry air is entrained from the FA into the BL (top left and right), which enhances the humidity excess but diminishes the temperature excess of updrafts.

In Fig. 3 horizontal cross sections through the thermal field displayed in Fig. 2 along a transect at $816\,m$ height are shown. The variations of temperature and moisture show similar structures as found by aircraft observations in the convective boundary layer [1], [2]. A variety of thermals can be seen like warm and moist updrafts or cool and dry updrafts which show, that the simple picture that updrafts are always related to positive temperature excess (being warmer than their environment) is not always true within a field of thermals.

Figure 4(a) shows vertical profiles of the mean temperature excess and the mean virtual temperature excess of all updrafts for the case Bo1_dq6. In order to investigate only updrafts that are usable for soaring, we included only updrafts with a vertical velocity $w < w_*$, where $w_* = (g/\overline{T}_0\,z_i\,B_s)^{1/3}$ is the so called convective velocity scale [3], [4], which indicates a typical updraft velocity for a given surface temperature $\overline{T}_0$, inversion

height z_i and surface buoyancy flux $B_s = (\overline{w'\,\theta_v'})_0$ which can be related to the sensible heat flux Q_s and latent heat flux Q_l by $B_s = a\,(Q_s + 0.07 Q_l)$, where $a = 1/(\rho\,c_p)$. It can be seen that the temperature differences between updrafts and their environment are in general very small (only about $0.1\,K$). The temperature excess decreases from more than $0.2\,K$ below $200\,m$ to less than $0.1\,K$ in the middle of the BL. At $z = z_T = 941\,m$ (or $0.73\,z_i$) the temperature excess is zero. However, at that height the updrafts are still positively buoyant (have a positive virtual temperature difference θ_v') due to the humidity difference between the updrafts and their environment (shown in Fig. 4(b). This humidity excess in the upper third of thermals has been also observed during inflight measurements of temperature and moisture by [3]. The buoyancy of updrafts becomes zero somewhat higher at $z = z_B = 1106\,m$ (or $0.85\,z_i$). The humidity excess of thermals is highest at the top of the updrafts, not because they gain humidity during their ascend but rather because the surrounding air is dryer at that height due to the entrainment of dry air from the FA. Temperature and virtual temperature differences become negative at the top of updrafts, reaching values of $-0.3\,K$.

In Fig. 5 the same profiles are shown as in Fig. 4 but for the case Bo0.1_dq6 (moist surface). Here, the temperature differences are smaller, but the influence of moisture on the virtual temperature excess (and hence on buoyancy) is more dominant as in the case with Bowen ratio $Bo = 1$. At $200\,m$ height, e.g., one half of the buoyancy is generated by temperature excess ($0.05\,K$) and one half is generated by humidity excess, so that a virtual temperature excess of $0.1\,K$ is obtained. In Fig. 6 these profiles are shown for the same Bowen ratio ($Bo = 1$) as in Fig. 4, but there is no jump of specific humidity ($\Delta q = 0$) at the inversion height. Here the influence of moisture on the temperature excess is quite small as compared to the result shown in Fig. 4, especially in the upper part of the BL. This shows, that the en-
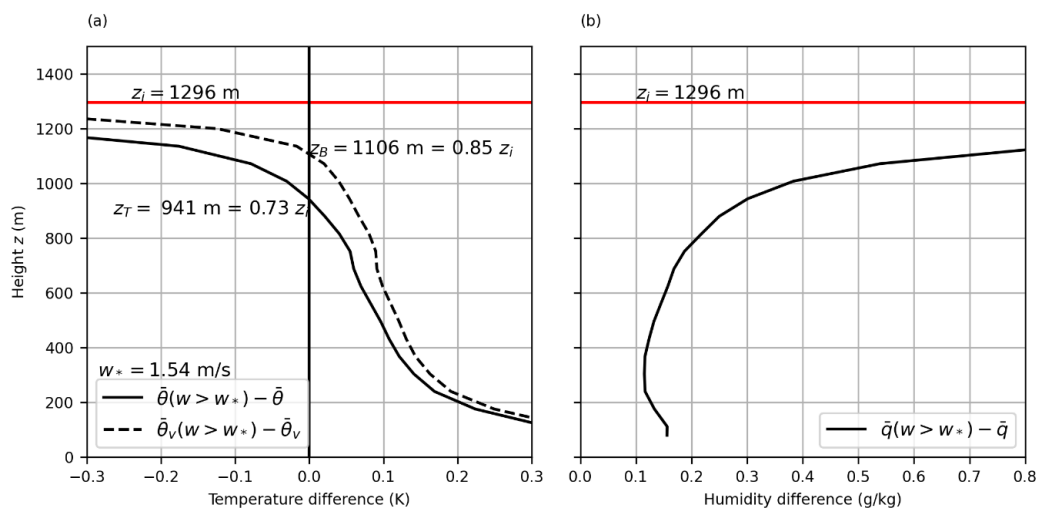

Fig. 4: Vertical profiles of temperature excess and virtual temperature excess (a) and humidity excess (b) of all updrafts that are stronger than w_* for the case Bo1_dq6
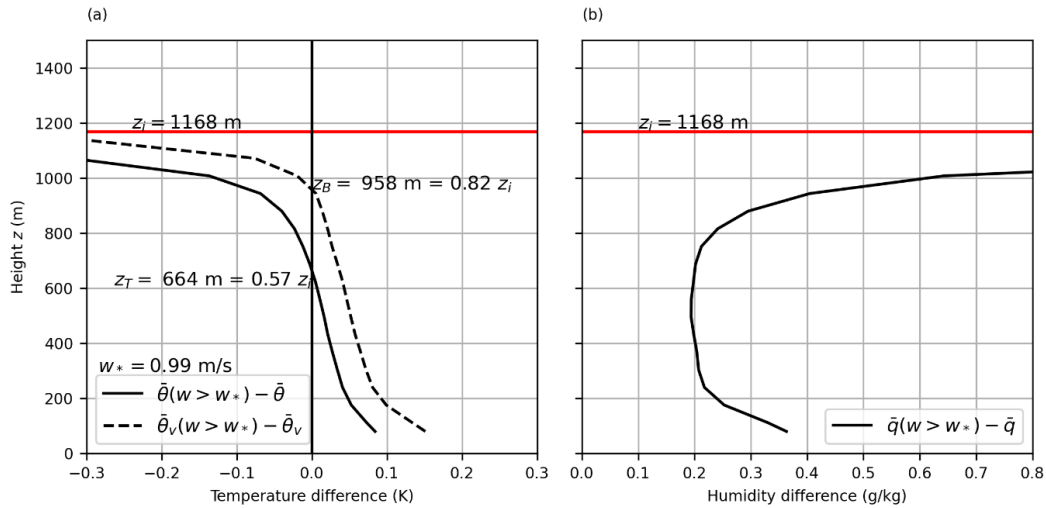
Fig. 5: Vertical profiles of temperature excess and virtual temperature excess (a) and humidity excess (b) of all updrafts that are stronger than w_* for the case Bo0.1_dq6.

Fig. 6: Vertical profiles of temperature excess and virtual temperature excess (a) and humidity excess (b) of all updrafts that are stronger than w_* for the case Bo1_dq0.
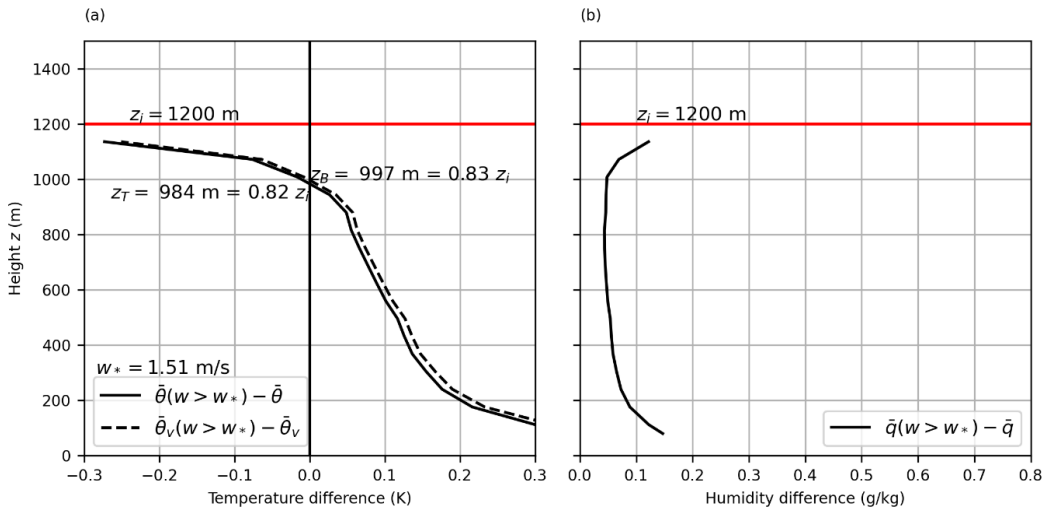
trainment of dry air from the FA above the inversion layer plays an important role on the influence of moisture on buoyancy, as can be seen by comparing the results with Fig. 4 and 5 and the summary of results in Table 1.

The heights for zero temperature excess z_T and zero buoyancy z_B of updrafts for all five cases are listed in Table 1. The updrafts reach zero buoyancy at about $0.85 z_i$, relatively independent of the Bowen ratio Bo and the humidity difference Δq between BL and FA. However, the height of zero temperature excess of updrafts z_T varies significantly and can be as low as $0.57 z_i$ for the case with $Bo = 0.1$ (wet surface). Note that in this case the updrafts are generally weaker (indicated by a small w_*), because most of the available surface heat flux is used for evaporation (latent heat flux), which is ineffective in generating

buoyancy. A large difference between z_B and z_T is achieved for wet surfaces ($Bo = 0.1$) and large humidity differences between BL and FA ($\Delta q = 11$) and nearly no difference between z_B and z_T is achieved for $\Delta q = 0$. Hence, the contribution of humidity on the buoyancy of updrafts is only dominant, if dry air is entrained from the FA into the BL. For very dry surfaces $Bo = 10$) or small humidity difference between BL and FA ($\Delta q = 0$), humidity effects play a minor role. In this case, the temperature excess of updrafts vanishes relatively late at $z_T = 0.80 z_i (Bo = 10)$ or $z_T = 0.82 z_i (\Delta q = 0)$.

Conclusions

With this study we showed that large-eddy simulation is a suitable method for the investigation of thermals, as the

spatiotemporal properties of thermals can be extracted while the boundary conditions can be controlled and systematically changed. The results show that updrafts become neutrally buoyant at about $0.85\,z_i$, more or less independent of Bowen ratio and humidity difference between the boundary layer and the free atmosphere. However, the temperature excess of updrafts becomes zero at heights between $0.57\,z_i$ and $0.82\,z_i$, with lower values for small Bowen ratios and high humidity differences. As humidity-driven buoyancy partly replaces temperature-driven buoyancy, humidity effects do not lead to stronger thermals but rather lead to colder thermals, for a given surface buoyancy flux. For a given surface heat flux, the strongest updrafts are achieved at high Bowen ratios (dry surfaces). The entrainment of dry air from a dry free atmosphere into a humid boundary layer significantly strengthens the upper part of updrafts.

It should be remembered however, that there is no water vapor condensation and hence cloud formation in our study. We wanted to focus on the direct effect of air moisture on buoyancy forces and hence on the formation of thermals. Once cloud formation is permitted, the indirect effect of moisture on the strength of thermals due to release of latent heat above the condensation level comes into play and can lead to stronger thermals than in the case without clouds. Important research topics for the future could be to study the effects of clouds, vegetation or wind on the structure of thermals.

References

[1] Kiessling, A., "Measurement results from warm air thermals over the Namibian steppe." *Proceedings XXXIV OSTIV Congress, Hosín, Czech Republic, 28 July – 3 August 2018*, 2018, pp. 126–129.

[2] Lenschow, D. H., "Aircraft Measurements in the Boundary Layer." *Probing the Atmospheric Boundary Layer*, edited by D. H. Lenschow, American Meteorological Society, Boston, MA, USA, 1986, pp. 39–55, `https://doi.org/10.1007/978-1-944970-14-7_5`.

[3] Predelli, O. and Niedernhagen, R., "Humidity, the dominating force of thermal updrafts." *Technical Soaring*, Vol. 45, No. 1, 2021, pp. 2–11.

[4] Schmidt, H. and Schumann, U., "Structure of the convective boundary layer derived from large-eddy simulations," *Technical Soaring*, Vol. 14, No. 4, 1990, pp. 118–123.

[5] Stoll, R., Gibbs, J. A., Salesky, S. T., Anderson, W., and Calaf, M., "Large-Eddy Simulation of the Atmospheric Boundary Layer." *Boundary-Layer Meteorology*, Vol. 177, 2020, pp. 541–581, `https://doi.org/10.1007/s10546-020-00556-3`.

[6] Patton, E. G., Sullivan, P. P., and Moeng, C.-H., "The Influence of Idealized Heterogeneity on Wet and Dry Planetary Boundary Layers Coupled to the Land Surface." *Journal of Atmospheric Sciences*, Vol. 62, 2005, pp. 2078–2097.

[7] Maronga, B. et al., "Overview of the PALM model system 6.0." *Geoscientific Model Development*, Vol. 13, No. 3, 2020, pp. 1335–1372, `https://doi.org/10.5194/gmd-13-1335-2020`.